Available online at www.sciencedirect.com
SCIENCE DIRECT®
Biochimica et Biophysica Acta 1557 (2003) 77–82
BIOCHIMICA ET BIOPHYSICA ACTA
BBA
www.bba-direct.com

^{18}O isotope effect in the photosynthetic water splitting process

Kvetoslava Burda[a,b], Klaus P. Bader[c], Georg H. Schmid[b,*]

[a] *Institute of Nuclear Physics, ul. Radzikowskiego 152, 31-342 Cracow, Poland*
[b] *Fakultät für Biologie, Lehrstuhl Zellphysiologie, Universität Bielefeld, Postafch 10 01 31, D-33501 Bielefeld, Germany*
[c] *Institut für Biomedizin und Umweltconsulting, Meisenstraße 96, 33607 Bielefeld, Germany*

Received 6 August 2002; received in revised form 28 November 2002; accepted 4 December 2002

Abstract

In mass spectroscopic experiments of oxygen evolution in Photosystem II at 50% enrichment of $H_2{}^{18}O$, one expects equal signals of $^{18}O_2$ and $^{16}O_2$ unless one of the isotopes is favored by the oxygen evolving complex (OEC). We have observed a deviation from this expectation, being a clear indication of an isotope effect. We have measured the effect to be 1.14–1.30, which is higher than the theoretically predicted value of 1.014–1.06. This together with the strong temperature variation of the measured effect with a discontinuity at 11 °C observed for wild-type tobacco and at 9 °C for a yellow-green tobacco mutant suggest that an additional mechanism is responsible for the observed high isotope effect. The entry of a finite size of water clusters to the cleavage site of the OEC can explain the observation.

Keywords: Photosystem II; Oxygen evolution; Mass spectrometer; Isotope effect

1. Introduction

Photosynthetic water oxidation occurring in thylakoid membranes of higher plants, algae and cyanobacteria is the only process which has enriched the formerly anaerobic atmosphere with oxygen up to the present level. It is Photosystem II (PS II) which is responsible for oxygen evolution [1]. Within recent years, our knowledge on PS II structure and function has increased significantly. It has been established that PS II is a multisubunit protein complex containing the intrinsic proteins D1, D2, CP47, CP43, cytochrome b_{559} and the extrinsic polypeptides 33, 23 and 17 kDa. These proteins are the major subunits associated with the oxygen evolving complex (OEC). It has been found that a manganese complex, bound to the D1 polypeptide [2], is the catalytic site for the conversion of water to molecular oxygen [3]. Among other inorganic cofactors, calcium and chloride ions were shown to be crucial for the proper functioning of the water splitting enzyme [4,5]. Water oxidation is a light-driven reaction [6]. Oxygen evolution measured as consequence of short saturating flashes has a periodicity of 4 which has been observed for the first time by Joliot et al. [7] and described by Kok et al. [8]. According to the Kok model, the water splitting complex cycles via subsequent five oxidation states S_i ($i=0$, 1, 2, 3, 4), where i denotes the number of accumulated charges. O_2 is evolved during the $S_3 \rightarrow (S_4) \rightarrow S_0$ transition.

Despite extensive studies of the OEC, the fundamental problem when and how water molecules enter and bind to the catalytic site is still open.

Recently growing experimental evidence supports the hypothesis of free access of water to the cleavage site of the water splitting enzyme independently of the redox states of the Mn complex. It has been estimated that water clusters that enter the cleavage site of the OEC contain in average 12 ± 2 water molecules [9]. Moreover, it has been shown by Evans et al. [10] that the exposure of the manganese complex to the aqueous environment is not homogenous. At the moment, it is not clear whether the water molecules occur in a bulk or whether they constitute structural water.

To get some direct insight into the mechanism of water splitting, we have made $H_2^{18}O$-labeled mass spectroscopic studies of oxygen evolution with thylakoids of two tobacco species differing in their thylakoid grana structure. Under the assumption of independent mixing of the labeled water, one expects that the equilibrium values of the mass spectroscopic signals 36:34:32 should be $\alpha^2{:}2\alpha(1-\alpha){:}(1-\alpha)^2$

Abbreviations: OEC; oxygen evolving complex

* Corresponding author. Tel.: +49-521-106-56-09; fax: +49-521-106-64-10.
E-mail address: G.Schmid@Biologie.Uni-Bielefeld.de (G.H. Schmid).

0005-2728/02/$ - see front matter © 2002 Elsevier Science B.V. All rights reserved.
doi:10.1016/S0005-2728(02)00395-X

independently of the temperature, where α is the ^{18}O-labeled water enrichment defined as the ratio of the $H_2{}^{18}O$ volume to the total ($H_2{}^{18}O + H_2{}^{16}O$) volume of water. The experiments have shown that this is not the case. There are two possible explanations for this experimental observation: (i) the cluster mechanism described in Ref. [9] and/or (ii) an oxygen-18 isotope effect. To disentangle the issue of the presence or absence of an isotope effect, we propose mass spectroscopic measurements with 50% enrichment of $H_2{}^{18}O$. For $\alpha = 0.5$, there is an entire symmetry between the fractions of ^{16}O and ^{18}O, namely, $^{18}O_2$:$^{16}O^{18}O$:$^{16}O_2 = 0.25:0.5:0.25$ and the system should react with both water species identically. Only if an isotope effect existed, asymmetry should occur.

2. Materials and methods

Thylakoid membranes were prepared from *Nicotana tabacum* var John William's Broadleaf (JWB) and from the yellow-green mutant *Su/su* using the procedure developed by Homann and Schmid [11] with slight modifications. Only freshly isolated thylakoids were used. Samples containing 100 μg chlorophyll in the case of wild-type tobacco and 50 μg chlorophyll in the case of the mutant were suspended in Tricine/KCl (0.06 M/0.03 M), pH 7.5.

The enrichment in labeled water $H_2{}^{18}O$ was always 50% in a final assay volume of 3 ml. $H_2{}^{18}O$ was obtained from CEA-Oris, Bureau des Isotopes Stables, Gif-sur-Yvette, France.

Oxygen evolution was measured in the presence of 1 mM ferricyanide by means of the mass-spectrometer 'type-Delta' from Finnigan MAT (Bremen, Germany) with a modified magnetic sector field. Details of the setup, adapted for these highly sensitive O_2 measurements are described in Refs. [12,13]. Thirty-two ($^{16}O_2$), 34 ($^{16}O^{18}O$) and 36 ($^{18}O_2$) signals induced in dark-adapted thylakoid membranes by excitation with 10 short saturating flashes spaced 300 ms apart were detected every 10 min after $H_2{}^{18}O$ injection. Flashes with a half-width of 5 μs were provided by the stroboscope 1539A from General Radio (xenon flash lamp).

The sample cell was cooled via connection to a thermostat. The temperature was kept constant within 0.1 °C.

To check the mixing process through diffusional relaxation induced by the fast injection of labeled water, we also measured the time-dependent mass spectroscopic signals 44 and 46 ($C^{18}O^{16}O$ and $C^{16}O_2$) in preparations containing 10 mM HCO_3^- and 100 units of carbonic anhydrase (dark reaction). We added 0.2 ml water enriched in 95.4% $H_2{}^{18}O$ into 2.133 ml sample containing $H_2{}^{16}O$. This is a standard procedure to determine the isotope enrichment in mass spectroscopic measurements when the spectrometer has low sensitivity [14]. In that case, there are usually problems in handling small quantities of isotope [14]. Our mass spectroscopic device is much more sensitive which permits the use of very low $H_2{}^{18}O$ labelings in direct measurements of oxygen evolution [13].

3. Results

We have studied time-dependent oxygen evolution in thylakoid membranes from wild-type tobacco and a yellow-green tobacco mutant in buffer containing 50% labeled water, as $H_2{}^{18}O$ ($\alpha = 0.5$). Measurements have been performed in a wide range of temperatures, from 4 to 22 °C. Typical mass spectroscopic signals at masses 32, 34 and 36

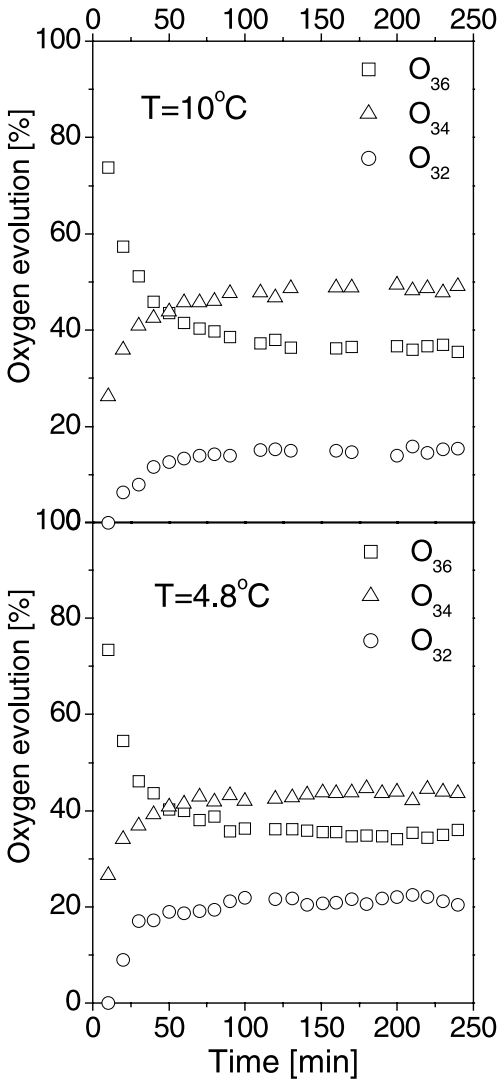

Values after equilibration:

T=10 °C	T=4.8°C
O_{36}=36.62 ± 0.21	O_{36}=35.29 ± 0.19
O_{34}=48.39 ± 0.23	O_{34}=43.43 ± 0.21
O_{32}=14.98 ± 0.15	O_{32}=21.37 ± 0.17

Fig. 1. Photosynthetic oxygen evolution in thylakoid membranes prepared from *N. tabacum* JBW. Ten short saturating flashes were given in intervals of 10 min. The measurement was started 10 min after the injection of $H_2{}^{18}O$. Shown are mass spectroscopic signals at masses 32, 34 and 36, the sum of which is normalized to 100%. The enrichment in labeled water ($H_2{}^{18}O$) was 50%.

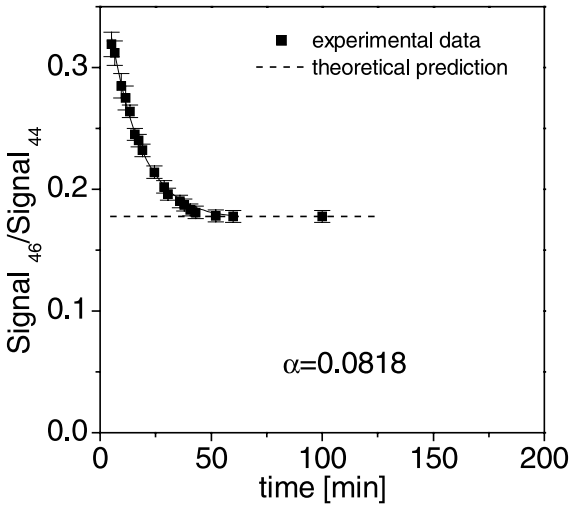

Fig. 2. Ratio of mass spectroscopic signals 46:44 corresponding to $C^{16}O^{18}O$:$C^{16}O_2$ as a function of time after the fast injection of $H_2{}^{18}O$. The solid line is a theoretical fit to the experimental data. The dashed line is the theoretical prediction of the ratio of signals 46 and 44 calculated from the binomial distribution for the applied enrichment $\alpha = 0.0818$ (the calculated ratio of these signals = 0.178).

for *N. tabacum* (JWB) thylakoids at 10 and 4.8 °C are shown in Fig. 1. If one assumes absence of an isotope effect, the ratio of the $^{18}O_2$:$^{18}O^{16}O$:$^{16}O_2$ signals should be 0.25:0.5:0.25 for $\alpha = 0.5$.

The experimental curves reach equilibrium after a number of repeatable short saturating flashes given at constant intervals of 10 min. This characteristic feature of the data can be explained theoretically by diffusional relaxation [9]. In fact, due to the fast injection of labeled water, the mass spectrometric signals 32, 34 and 36 reach the equilibrium value P_{eq} much faster than expected for pure diffusion. Clearly, the determined equilibrium state is reached only after the mixing process is completed. In Fig. 2, we present the ratio of the signals 46:44 ($C^{18}O^{16}O$ and $C^{16}O_2$), which is a very sensitive parameter of the real enrichment in the sample [14]. The diffusional process led to equilibrium within 50 min (at 20 °C) after the injection of labeled water, as has been also observed for the O_2 signals (Ref. [9] and this work). The reached equilibrium state for the signals 44 and 46 corresponds to the theoretical predictions according to the binomial distribution (Fig. 2). However, the ratios of the signals 36:34:32 for the steady states differ from the theoretical ratio 0.25:0.5:0.25 for the case of 50% enrichment, which means that the OEC distinguishes these two oxygen isotopes.

To quantify the effect, we introduce the concept of effective enrichment (α_{eff}) — a quantity defined by the best fit to the experimental results from the formula:

$$^{36}P_{eq}:^{34}P_{eq}:^{32}P_{eq} = \alpha_{eff}^2 : 2\alpha_{eff}(1-\alpha_{eff}) : (1-\alpha_{eff})^2. \quad (1)$$

This corresponds to the ^{18}O enrichment felt by the OEC. The effective enrichment α_{eff} can be calculated from Eq. (1) which when solved for α_{eff} gives:

$$\alpha_{eff} = \frac{2\,^{36}P_{eq} + {}^{34}P_{eq}}{2} \quad (2)$$

or alternatively, as described in Ref. [9], from the ratio of the average cluster size entering the reaction pocket and of the average number of $H_2^{18}O$ molecules in the cluster. In Fig. 3,

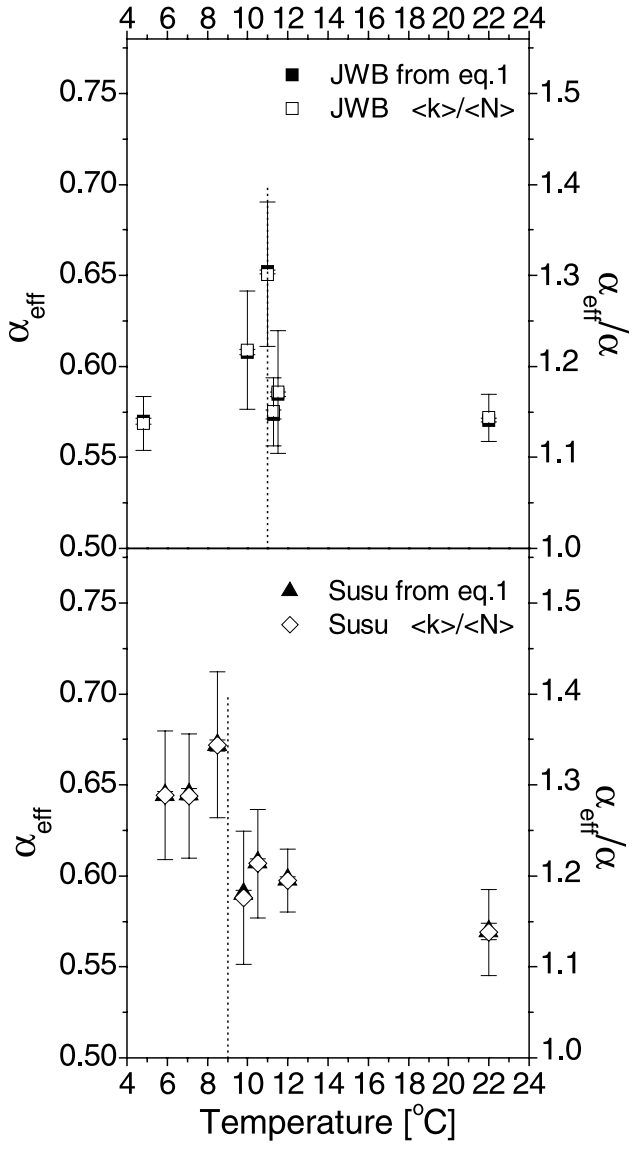

Fig. 3. Temperature dependence of the effective enrichment α_{eff} (values are given on the left scale), felt by the studied systems (thylakoid membranes from *N. tabacum* JWB and from the yellow-green mutant *Su/su*) and of the experimentally observed isotope effect estimated from α_{eff}/α, where $\alpha = 0.5$ (values are given on the right scale). The samples contained 50% of $H_2{}^{18}O$. α_{eff} is calculated from Eq. (2) or from the ratio $\langle k\rangle/\langle N\rangle$, where $\langle N\rangle$ is the average number of the water molecules in the water cluster entering the reaction pocket and $\langle k\rangle$ is the number of $H_2{}^{18}O$ molecules in the cluster. Note, that the error bars for the data displayed by triangles are of the symbol size.

we show the effective concentrations α_{eff} for wild-type and yellow-green tobacco. For both tobacco species, the experimentally obtained $H_2^{18}O$ enrichment varies with the temperature exhibiting a transition temperature at 11 °C for the wild type and at 9 °C for the yellow-green tobacco mutant.

In the calculations, we took into account the effect of an oxygen consumption within the examined systems. It varied usually between 4% and 10% of the total O_2 yield.

4. Discussion

The observed asymmetry of the equilibrium signals for $^{32}P_{eq}$ and $^{36}P_{eq}$ (see Fig. 1) indicates that the system prefers to evolve $^{18}O_2$. Experimental conditions were settled in such a way as to ensure no preferential factors for any oxygen species. Thus, the existence of an asymmetry can be only attributed to an intrinsic preference of the OEC for one of the isotopes, that is to an isotope effect. The ratio of α_{eff}/α is a measure of the experimentally observed isotope effect (see Fig. 3). The observed effect is very strong. We compare it to the equilibrium constant for an isotope exchange, K_{eq}, which plays a role similar to the ratio α_{eff}/α.

In case of the water splitting enzyme, the manganese complex takes part as an intermediate in the process of oxygen yield (for review, see Refs. [15–17]). Assuming the existence of an intermediate stage E, which is related to the Mn cluster: $E + 2H_2O \leftrightarrow E(2H_2O) \rightarrow E(2O) + 4e^- + 4H^+ \rightarrow E + O_2 + 4e^- + 4H^+$, the isotope equilibrium constant can be calculated as follows:

$$K_{eq}^{18} = \left(\left[\frac{f(^{18}O_2)}{f(^{16}O_2)} \right] \Big/ \left[\frac{f(E^{*18}O)}{f(E^{*16}O)} \right]^2 \right) \times \left(\left[\frac{f(E^{*18}O)}{f(E^{*16}O)} \right] \Big/ \left[\frac{f(H_2{}^{18}O)}{f(H_2{}^{16}O)} \right] \right). \quad (3)$$

The square power results from the stoichiometry of the reaction $2(E{\cdot}O) \rightarrow O_2$. The equilibrium constant depends on the ratios of isotopic partition functions (f^{18}/f^{16}) of the participating chemical molecules. The partition functions for diatomic and polyatomic molecules were calculated in the quantum approximation of harmonic oscillators as a function of their frequencies according to Urey and Grieff [18]. Table 1 contains the vibrational frequencies of chosen synthesized compounds, being model systems of the OEC. The compounds consist of dinuclear or tetranuclear Mn components possessing mixed-valence manganese μ-oxo bridges [24–26,28]. These compounds have been found to undergo one- or two-redox conversions and some of them are able to evolve oxygen [29,30]. It is believed that dioxygen binding O—O occurs at di- or tetranuclear Mn complexes through the coupling of μ-oxo bridges [15] or the formation of peroxo bridges [31,32]. In the latter case, one of the Mn cations can be exchanged by other residues (e.g. histidine) [33,34], which could be active during the water

Table 1
Vibrational frequencies (cm^{-1}) and ratios of partition functions (f^{18}/f^{16})

Molecule	Mode	Vibrational frequencies		f^{18}/f^{16}	
		ν_{16}	ν_{18}	279 K	300 K
O_2[a]		1556	1467	1.689	1.662
H_2O[b]	H—O	3834	3821[t]		
	H—O	3943	3934[t]	1.29	1.28
	H—O—H	1647	1641[t]		
Mn cluster of the OEC[c]	Mn—O—Mn	606	579[t]	1.230	1.226
$[Mn_2O_2(pbz)_4]^{3+}$ $[Mn_2O_2(pbz)_4]^{4+}$[d]	$[Mn^{III/IV}\mu{-}O]_2^{+3}$	694(3)	665(4)	1.237	1.232
$[Mn_2O(O_2CCH_3)_2(HBpz_3)_2]$[e]	$Mn^{III}—O—Mn^{III}$	558	541	1.275	1.265
		717	680		
$[Mn(O)\eta^4\text{-}R_{1-4}]^-$[f]	$Mn^V \equiv O$	975.5	937	1.267	1.259
Mn^{III}HRP[g]	$Mn^{IV}=O$	622	592	1.268	1.263

Index [t] means that ν_{18} is calculated from the formula $\nu_{18}=(\mu_{18}/\mu_{16})^{1/2}\nu_{16}$, where μ_i is the reduced mass of a component containing ^{18}O or ^{16}O, respectively. All other values are experimental data.

pbz = 2-(2-pyridyl) benzimidazole.

$HBpz_3^-$ = hydrotris (1-pyrazolyl) borate.

MnHRP = manganese-substituted horseradish peroxidase.

[a] ν_{16} taken from Ref. [19].

[b] ν_{16} from Ref. [20].

[c] ν_{16} from Ref. [21].

[d] ν_{16} and ν_{18} from Ref. [22].

[e] ν_{16} and ν_{18} from Ref. [23], similar streching bands at 560 and 700 cm^{-1} have been observed for $[(H_2O)Mn^{III}(\mu\text{-}O)\text{-}(\mu O_2CR)_2Mn^{III}(L)]$, where $L = CrO_7^{2-}$, CH_3OH) by Dave and Czernuszewicz [24].

[f] Average of ν_{16} and ν_{18} for different manganyls [25], where R_{1-4} are different tetradeprotonated tetraamide macrocycles described in Refs. [25,26].

[g] ν_{16} and ν_{18} from Ref. [27].

splitting mechanism according to the model proposed in Ref. [29].

We give the ratios of the partition functions estimated for two different temperatures (279 and 300 K) in Table 1. It is interesting to note that the ratios of partition functions for compounds with Mn−O (=O) bonds are only slightly smaller (by about 1–4%) than for a water molecule with H−O bonds. Such small differences result from the fact that a decrease of the force constant for Mn−O in comparison with H−O is compensated by an increase of the mass (Mn vs. H) in the partition function.

The values of isotopic equilibrium constants calculated according to the formula (3) are given in Table 2. In the most simple case when we consider a direct equilibrium between O_2 and $2H_2O$, the isotopic exchange equilibrium is expressed by:

$$K_{eq}^{18} = \left[\frac{f(^{18}O_2)}{f(^{16}O_2)}\right] \Big/ \left[\frac{f(H_2{}^{18}O)}{f(H_2{}^{16}O)}\right]^2. \quad (4)$$

Thus, as can be seen from Table 2, an isotope effect should be of the order of 1.014 at room temperature. Introduction of the intermediate state E [as discussed above (see Eq. (3))] into the estimation of the equilibrium isotope effect increases K_{eq} even up to 1.06. However, this is not sufficient, because the experimental isotope effect measured as the ratio α_{eff}/α is much stronger than the theoretically predicted one and varies between 1.14 and 1.30 for both types of tobacco. We want to emphasize that the effect is independent on the $H_2^{18}O$ enrichment (see Fig. 3 in Ref. [9]). The isotope effect changes due to differences of force constants between reactant and transition states at the site of isotopic substitution. The accumulation of the heavier isotope, in our case of ^{18}O or ^{15}N as in the case of the earlier described hydroxylamine oxidation in tobacco chloroplasts (IE = 1.05) [35], can be observed when the force constant tends to be larger. On first sight, it might look plausible that a kinetic isotope effect is responsible for the difference between the theoretical and experimental isotope effect, but in general, kinetic heavy atom effects are small in comparison to equilibrium isotope effects [36].

There is no doubt that the observed effect is an intrinsic feature of the water splitting system which shows a discontinuity at 11 °C for wild-type tobacco and at about 9 °C for the yellow-green tobacco mutant. One sees from the temperature-dependent part of the partition function that the isotope effect should only weakly decrease with temperature [37]. However, at the transition temperatures, the observed effect increases two times. It is rather unusual to observe such significant changes of an isotope effect in such a narrow temperature range and therefore we expect that an additional mechanism within the OEC takes place, which depends on the structure of the lamellar system. In fact, the idea that the observed amplification of the isotope effect is due to a temperature-dependent rearrangement of the whole catalytic site (we mean conformational changes of the protein matrix), affecting water accessibility to the cleavage site of the water splitting enzyme, is very attractive. It would be consistent with the observed temperature changes of *S*-state populations, of the transitions between them and the modes of O_2 yield [38,39] as well as with the temperature dependence of the kinetic H/D isotope exchange effect on univalent oxidation steps of OEC PS II membrane fragments, studied by absorption changes on the donor side [40]. The detected discontinuities at 11 °C are in agreement with our mass spectroscopic data. The changes in hydrophilic properties at the catalytic site may be responsible for the heterogeneity described in Refs. [38,41].

A similar isotope effect to the one discussed in this paper was observed in the EPR measurements of Hansson et al. [42]. A simulation of the S_2 EPR signal with less than six water ligands has given a good agreement with the experimental data only for an unrealistic high enrichment ≥ 50% in comparison with the applied one 42%. This makes the isotope effect to be larger than 1.19 (IE ≥ (0.5/0.42) ≥ 1.19).

In conclusion, the presence of an isotope effect is not sufficient to explain the strong deviations of the isotope distribution of oxygen molecules at equilibrium from the values 0.25:0.5:0.25 expected from Eq. (1) for 50% $H_2{}^{18}O$ enrichment. We postulate that the mechanism that underlies this effect, leading to an amplification of the isotope effect, is due to a clustering of water molecules at the catalytic site. The water cluster should be understood as a hydration sphere of metal ion(s) (most probably Ca^{2+} and/or Mn^{2+} [43]) and it is known from the studies on water exchanges between hydrated cations and solvent water that cations have greater affinity for $H_2{}^{18}O$ than for $H_2{}^{16}O$ [44].

Table 2
Calculated equilibrium constants of isotope exchange

Intermediate state	Mode	$^{18}K_{eq}$	
		279 K	300 K
Directly from H_2O		1.015	1.014
Mn cluster of the OEC	Mn−O−Mn	1.064	1.059
$[Mn_2O_2(pbz)_4]^{3+}$ $[Mn_2O_2(pbz)_4]^{4+}$	$[Mn^{III/IV}\mu-O]_2^{+3}$	1.058	1.054
$[Mn_2O(O_2CCH_3)_2(HBpz_3)_2]$	$Mn^{III}-O-Mn^{III}$	1.027	1.026
$[Mn(O)\eta^4\text{-}R_{1-4}]^{-}$ [a]	$Mn^{V}\equiv O$	1.033	1.031
Mn^{III}HRP	$Mn^{IV}=O$	1.032	1.028

pbz = 2-(2-pyridyl) benzimidazole.
$HBpz_3^-$ = hydrotris (1-pyrazolyl) borate.
MnHRP = manganese-substituted horseradish peroxidase.
[a] R_{1-4} are different tetradeprotonated tetraamide macrocycles described in Refs. [25,26].

Acknowledgements

K.B. acknowledges the award of a stipendium from the Deutscher Akademischer Austauschdienst (DAAD). The skillful technical assistance of. Mrs. Kristina Neudorf is also

acknowledged. This work was partially supported by KBN grant 6 P04A 03817.

References

[1] G. Renger, Biochim. Biophys. Acta 1503 (2001) 210–228.
[2] A. Zouni, K.T. Witt, J. Kern, P. Fromme, N. Krauß, W. Saenger, P. Orth, Nature 409 (2001) 739–743.
[3] B.A. Diner, Biochim. Biophys. Acta 1503 (2001) 147–163.
[4] R.J. Debus, Biochim. Biophys. Acta 1102 (1992) 269–352.
[5] G.M. Ananyev, L. Zaltsman, C. Vasko, G.C. Dismukes, Biochim. Biophys. Acta 1503 (2001) 52–68.
[6] G. Renger, Photosynth. Res. 38 (1993) 229–247.
[7] P. Joliot, G. Barbieri, R. Chabaud, Photochem. Photobiol. 10 (1969) 309–329.
[8] B. Kok, B. Forbusch, M. McGloin, Photochem. Photobiol. 11 (1970) 457–475.
[9] K. Burda, K.P. Bader, G.H. Schmid, FEBS Lett. 491 (2001) 81–84.
[10] M.C.W. Evans, K. Gourovskaya, H.A. Nugent, FEBS Lett. 450 (1999) 285–288.
[11] P.H. Homann, G.H. Schmid, Plant Physiol. 42 (1967) 1619–1632.
[12] K.P. Bader, P. Thibault, G.H. Schmid, Biochim. Biophys. Acta 893 (1987) 564–571.
[13] K.P. Bader, G.H. Schmid, Biochim. Biophys. Acta 1456 (2000) 108–120.
[14] R. Radmer, O. Ollinger, FEBS Lett. 110 (1980) 57–61.
[15] V.K. Yachandra, K. Sauer, M.P. Klein, Chem. Rev. 96 (1996) 2927–2950.
[16] M. Haumann, W. Junge, Biochim. Biophys. Acta 1411 (1999) 86–91.
[17] G. Renger, in: G.S. Singhal, G. Renger, S.K. Sopary, K.D. Irrgang, Govindjee (Eds.), Concepts of Photosynthesis and Photogenesis, Narosa Publishing House, New Delhi, 1999, pp. 292–329.
[18] H.C. Urey, L.J. Greiff, J. Am. Chem. Soc. 1 (1935) 321–327.
[19] M.W. Chase, J.L. Doewney, J.R. McDonald, R.A. Syverud, E.A. Valenzuela, J. Phys. Chem. Ref. Data 11 (1982) 695–740.
[20] M.G. Bucknell, N.C. Handy, Mol. Phys. 28 (1974) 777–792.
[21] H.A. Chu, W. Hillier, N.A. Low, G.T. Babcock, Biochim. Biophys. Acta 1503 (2001) 69–82.
[22] B.C. Dave, R.S. Czernuszewicz, Inorg. Chim. Acta 227 (1994) 33–41.
[23] J.E. Sheats, R.S. Czernuszewicz, G.C. Dismukes, A.L. Rheingold, V. Petrouleas, J. Stubbe, W.H. Armstrong, R.H. Beer, S.J. Lippard, J. Am. Chem. Soc. 109 (1987) 1433.
[24] B.C. Dave, R.S. Czernuszewicz, Inorg. Chim. Acta 281 (1998) 25–35.
[25] J.M. Workman, R.D. Powell, A.D. Procyk, T.J. Collins, D.F. Bocian, Inorg. Chem. 31 (1992) 1548–1550.
[26] T.J. Collins, R.D. Powell, C. Slebodnick, E.S. Uffelman, J. Am. Chem. Soc. 113 (1991) 8419–8425.
[27] R.J. Nick, G.B. Ray, K.M. Fish, T.G. Spiro, T.J. Groves, J. Am. Chem. Soc. 113 (1991) 1838–1840.
[28] M.J. Baldwin, A. Gelasco, V.L. Pecoraro, Photosynth. Res. 38 (1993) 303–308.
[29] J. Limburg, J.S. Vrettos, H. Chen, J.C. de Paula, R.H. Crabtree, G.W. Brudvig, J. Am. Chem. Soc. 123 (2001) 423–430.
[30] W. Ruettinger, M. Yagi, K. Wolf, S. Brnasek, G.C. Dismukes, J. Am. Chem. Soc. 122 (2000) 10353–10357.
[31] B.C. Dave, R.S. Czernuszewicz, New J. Chem. 18 (1994) 149–155.
[32] Govindjee, T. Kambara, W.R. Coleman, Photochem. Photobiol. 42 (1985) 187–210.
[33] A. Boussac, J.L. Zimmermann, A.W. Rutherford, J. Lavergne, Nature 347 (1990) 303–306.
[34] R.J. Debus, K.A. Campbell, J.M. Peloqiun, D.P. Pham, R.D. Britt, Biochemistry 39 (2000) 470–478.
[35] G. Renger, K.P. Bader, G.H. Schmid, Biochim. Biophys. Acta 1015 (2000) 288–294.
[36] W.A. van Hook, in: C.J. Collins, N.S. Bowman (Eds.), Isotope Effects in Chemical Reactions, Van National Reinhold Company, Canada, 1970, pp. 1–89.
[37] J.P. Klinman, Adv. Enzymol. 46 (1978) 415–495.
[38] K. Burda, G.H. Schmid, Biochim. Biophys. Acta 1506 (2001) 47–54.
[39] K. Burda, P. He, K.P. Bader, G.H. Schmid, Z. Naturforsch. 51c (1996) 823–832.
[40] M. Karge, K.D. Irrgang, G. Renger, Biochemistry 36 (1997) 8904–8913.
[41] K. Burda, G.H. Schmid, Z. Naturforsch. 51c (1996) 329–341.
[42] Ö. Hansson, L.E. Andreasson, T. Vänngård, FEBS Lett. 195 (1986) 151–154.
[43] M.L. Latimer, V.J. DeRose, I. Mukerji, V.K. Yachandra, K. Sauer, M.P. Klein, Biochemistry 34 (1995) 10898–10909.
[44] J.P. Hunt, H. Taube, J. Chem. Phys. 19 (1951) 602–609.